Measuring changes in *Plasmodium falciparum* census population size in response to sequential malaria control interventions

Kathryn E. Tiedje[1,2§], Qi Zhan[3,4§], Shazia Ruybal-Pésantez[2†], Gerry Tonkin-Hill[2,5], Qixin He[4‡], Mun Hua Tan[1], Dionne C. Argyropoulos[1], Samantha L. Deed[1,2], Anita Ghansah[6], Oscar Bangre[7], Abraham R. Oduro[7], Kwadwo A. Koram[8], Mercedes Pascual[9,10], and Karen P. Day[1,2]

[1] Department of Microbiology and Immunology, Bio21 Institute and Peter Doherty Institute for Infection and Immunity, The University of Melbourne; Melbourne, Australia
[2] School of BioSciences, Bio21 Institute, The University of Melbourne; Melbourne, Australia
[3] Committee on Genetics, Genomics and Systems Biology, The University of Chicago; Chicago, Illinois, USA
[4] Department of Ecology and Evolution, The University of Chicago; Chicago, Illinois, USA
[5] Bioinformatics Division, Walter and Eliza Hall Institute; Melbourne, Australia
[6] Department of Parasitology, Noguchi Memorial Institute for Medical Research, University of Ghana; Legon, Ghana
[7] Navrongo Health Research Centre, Ghana Health Service; Navrongo, Ghana
[8] Epidemiology Department, Noguchi Memorial Institute for Medical Research, University of Ghana; Legon, Ghana
[9] Department of Biology and Department of Environmental Sciences, New York University, New York, New York, USA
[10] Santa Fe Institute, Santa Fe, New Mexico, USA

† *Current affiliations:* Department of Infectious Disease Epidemiology and MRC Centre for Global Infectious Disease Analysis, School of Public Health, Imperial College London, United Kingdom

‡ *Current affiliation:* Department of Biological Sciences, Purdue University; West Lafayette, United States

§ These authors share first authorship

* Corresponding Author: Karen P. Day, Department of Microbiology and Immunology, Bio21 Institute and Peter Doherty Institute for Infection and Immunity, The University of Melbourne, 30 Flemington Road, Parkville, VIC, 3011, Australia. E-mail: Karen.Day@unimelb.edu.au, Phone: +613 8344 2377

RUNNING TITLE: Impact of IRS and SMC on census population size

ABSTRACT

Here we introduce a new endpoint "census population size" to evaluate the epidemiology and control of *Plasmodium falciparum* infections, where the parasite, rather than the infected human host, is the unit of measurement. To calculate census population size, we rely on a definition of parasite variation known as multiplicity of infection (MOI_{var}), based on the hyper-diversity of the *var* multigene family. We present a Bayesian approach to estimate MOI_{var} from sequencing and counting the number of unique DBLα tags (or DBLα types) of *var* genes, and derive from it census population size by summation of MOI_{var} in the human population. We track changes in this parasite population size and structure through sequential malaria interventions by indoor residual spraying (IRS) and seasonal malaria chemoprevention (SMC) from 2012 to 2017 in an area of high-seasonal malaria transmission in northern Ghana. Following IRS, which reduced transmission intensity by > 90% and decreased parasite prevalence by ~40-50%, significant reductions in *var* diversity, MOI_{var}, and population size were observed in ~2,000 humans across all ages. These changes, consistent with the loss of diverse parasite genomes, were short lived and 32-months after IRS was discontinued and SMC was introduced, *var* diversity and population size rebounded in all age groups except for the younger children (1-5 years) targeted by SMC. Despite major perturbations from IRS and SMC interventions, the parasite population remained very large and retained the *var* population genetic characteristics of a high-transmission system (high *var* diversity; low *var* repertoire similarity) demonstrating the resilience of *P. falciparum* to short-term interventions in high-burden countries of sub-Saharan Africa.

INTRODUCTION

Malaria in high-transmission endemic areas of sub-Saharan Africa (SSA) is characterised by vast diversity of the *Plasmodium falciparum* parasites from the perspective of antigenic variation (Chen et al., 2011; Day et al., 2017; Otto et al., 2019; Ruybal-Pesántez et al., 2022, 2017). As with other hosts of hyper-variable pathogens (Futse et al., 2008), children experiencing clinical episodes of malaria, eventually become immune to disease but not to infection. This results in a large reservoir of chronic asymptomatic infections, in hosts of all ages, sustaining transmission to mosquitos. Given the goal of malaria eradication by 2050, it is therefore of interest to examine how the parasite population changes following perturbation by major intervention efforts, both in terms of its size and underlying population genetics.

So, what do we mean by the parasite population size in the case of *P. falciparum* and how do we measure it? Parasite prevalence, detected by microscopy or more sensitive molecular diagnostics (e.g., PCR), describes the proportion of infected human hosts. Studies of *P. falciparum* genetic diversity have shown that the majority of people in high-transmission endemic areas harbour diverse multiclonal infections measured as the complexity or multiplicity of infection (MOI) (e.g., (Anderson et al., 2000; Paul et al., 1995; Smith et al., 1999; Sumner et al., 2021)) with complex population dynamics (Bruce et al., 2000; Farnert et al., 1997). These genetic data indicate much larger parasite population sizes than observed by prevalence of infection alone. Thus, from an ecological perspective, we can consider a human host as a patch carrying a number of "antigenically-distinct infections" of *P. falciparum*. The sum of these antigenically-distinct infections over all sampled hosts provides us with a census of the parasite count of relevance to monitoring and evaluating malaria interventions. We refer to this census population size hereafter simply as population size but make clear that this measure is distinct from effective population

size (N_e) as measured by neutral variation. This count can be scaled from the host sample to the larger denominator of a host population in the area of interest.

Diversity of *P. falciparum* single copy surface antigen genes such as circumsporozoite protein (*csp*), merozoite surface protein 1 (*msp1*) or 2 (*msp2*), and apical membrane antigen 1 (*ama1*) have each been widely used to measure MOI (e.g., (Falk et al., 2006; Lerch et al., 2017; Nelson et al., 2019)). They have become part of newer genetic panels (e.g., Paragon v1 (Tessema et al., 2020) and AMPLseq v1 (LaVerriere et al., 2022)) specifically for MOI determination. Typically, MOI is reported as the maximum number of alleles or single locus haplotypes present at the most diverse of these antigen-encoding loci rather than the number of unique multilocus haplotypes of these genes combined, as it is challenging to accurately reconstruct or phase these haplotypes in hosts with an MOI > 3 (Lerch et al., 2019). Each of these genes is under balancing selection with a few geographically-common haplotypes and many very rare haplotypes in moderate- to high-transmission settings (Markwalter et al., 2022; Sumner et al., 2021). Where there is a high probability of co-occurrence of two or more common single locus haplotypes in a host, genotyping each of these single copy antigen genes alone will underestimate MOI. Single nucleotide polymorphism (SNP) panels have been used to define the presence of multiclonal infections with limited reliability to estimate MOI for highly complex infections, typical in high transmission, even with the use of computational methods (Labbé et al., 2023).

As an alternative to genotyping single copy antigen genes and biallelic SNP panels to estimate MOI, we have proposed the use of a fingerprinting methodology known as *var*coding to genotype the hyper-diverse *var* multigene family (~50-60 *var* genes per haploid genome). This method employs a ~450bp region of a

101 *var* gene, known as a DBLα tag encoding the immunogenic Duffy-binding-like alpha (DBLα) domain of
102 PfEMP1 (*Plasmodium falciparum* erythrocyte membrane protein 1), the major surface antigen of the
103 blood stages (Zhang and Deitsch, 2022). Bioinformatic analyses of a large database of exon 1 sequences
104 of *var* genes showed a predominantly 1-to-1 DBLα-*var* relationship, such that each DBLα tag typically
105 represents a unique *var* gene, especially in high transmission (Tan et al., 2023). The extensive diversity of
106 DBLα tags together with the very low percentage of *var* genes shared between parasites (Chen et al.,
107 2011; Day et al., 2017; Ruybal-Pesántez et al., 2022, 2017) facilitate measuring MOI by amplifying, pooling,
108 sequencing, and counting the number of unique DBLα tags (or DBLα types) in a host (Ruybal-Pesántez et
109 al., 2022; Tiedje et al., 2022). From a single PCR with degenerate primers and amplicon sequencing, the
110 method specifically counts the most diverse DBLα types, designated non-upsA, per infection to arrive at
111 a metric we call MOI_{var}. It is not based on assigning haplotypes but exploits the fact that *var* repertoires
112 are non-overlapping, especially in high transmission. Instead, it assumes a set number of non-upsA types
113 per genome based on repeated sampling of 3D7 control isolates accounting for PCR sampling errors to
114 calculate MOI_{var} (Ghansah et al., 2023; Ruybal-Pesántez et al., 2022; Tiedje et al., 2022). Consequently,
115 rather than looking at the diversity of a single copy antigen-encoding gene like *csp, msp2,* or *ama1* to
116 calculate MOI, by *var*coding we are looking at sets of up to 45 non-upsA DBLα types per genome. Prior
117 work has shown that *var*coding is more sensitive to measure MOI in high transmission where there is an
118 extremely high prevalence of multiclonal infections that cannot be accurately phased with either biallelic
119 SNP panels (Ghansah et al., 2023; Labbé et al., 2023; Tessema et al., 2020; Watson et al., 2021) or
120 combinations of single copy antigen genes (Sumner et al., 2021).
121

122 Here we report an investigation of changes in parasite census population size and structure through two
123 sequential malaria control interventions between 2012 and 2017 in Bongo District located in the Upper
124 East Region of Ghana, one of the 12 highest burden countries in Africa (World Health Organization, 2022).
125 We present a novel Bayesian modification to the published *var*coding approach (Ghansah et al., 2023;
126 Ruybal-Pesántez et al., 2022; Tiedje et al., 2022) that takes into account under-sampling of non-upsA DBLα
127 types in an isolate to estimate MOI_{var} (Ruybal-Pesántez et al., 2022; Tiedje et al., 2022) and therefore
128 population size. We document *P. falciparum* prevalence as well as *var* diversity and population structure
129 from baseline in 2012 through a major perturbation by a short-term indoor residual spraying (IRS)
130 campaign managed under operational conditions, which reduced transmission intensity by > 90% as
131 measured by the entomological inoculation rate (EIR) and decreased parasite prevalence by ~40-50%
132 (Tiedje et al., 2022). Next, we followed what happened to parasite population size more than two years
133 after the IRS intervention was discontinued and seasonal malaria chemoprevention (SMC) was introduced
134 for children between the ages of 3-59 months (i.e., < 5 years) (Wagman et al., 2018). Detectable changes
135 in parasite population size were seen as a consequence of the IRS intervention but this quantity rapidly
136 rebounded 32-months after the intervention ceased. Overall, throughout the IRS, SMC, and subsequent
137 rebound, the parasite population in humans remained large in size and retained the *var* population
138 genetic characteristics of high transmission (i.e., high *var* diversity, low *var* repertoire overlap),
139 demonstrating the overall resilience of the species to survive significant short-term perturbations.

140 # MATERIALS AND METHODS

141 ## Human subject ethical approval

142 The study was reviewed/approved by the ethics committees at the Navrongo Health Research Centre
143 (Ghana), Noguchi Memorial Institute for Medical Research (Ghana), The University of Melbourne
144 (Australia), The University of Chicago (United States), and New York University (United States). Details on
145 the study area, study population, inclusion/exclusion criteria, and data collection procedures have been
146 previously described (Tiedje et al., 2022, 2017).

147

148 ## Study design and sample collection

149 Using an interrupted time-series study design, four age-stratified cross-sectional surveys of ~2,000
150 participants per survey were undertaken to investigate the impacts of IRS and SMC in combination with
151 long-lasting insecticidal nets (LLINs) impregnated with pyrethroids under operational conditions on the
152 asymptomatic *P. falciparum* reservoir from two proximal catchment areas (i.e., Vea/Gowrie and Soe, with
153 a sampling area of ~60 km^2) in Bongo District, Ghana (hereinafter referred to collectively as "Bongo";
154 (Tiedje et al., 2022, 2017)) (Table supplement 1). Bongo District, located in the Upper East Region, is
155 categorized as high-seasonal malaria transmission based on the World Health Organization's (WHO) "A
156 Framework for Malaria Elimination" (WHO/GMP, 2017) where *P. falciparum* prevalence was ≥ 35% at
157 baseline in 2012 (Tiedje et al., 2022, 2017). These ~2,000 participants of all ages (1-97 years) represent
158 ~15% of the total population that reside in these two catchment areas in Bongo (Tiedje et al., 2017). The
159 four cross-sectional surveys were completed at the end of the wet season (i.e., high-transmission season)
160 and the study can be separated into four distinct study time points: (1) October 2012 (Survey 1) prior to
161 the IRS and SMC (i.e., baseline), (2) October 2014 (Survey 2) two months after the second round of IRS

162 (Actellic 50EC), (3) October 2015 (Survey 3) seven months after the third round of IRS using a long-acting
163 non-pyrethroid insecticide (Actellic 300CS) (Gogue et al., 2020; US President's Malaria Initiative Africa IRS
164 (AIRS) Project, 2016), and finally (4) October 2017 (Survey 4) 32-months after the discontinuation of IRS,
165 but during the deployment of SMC to all children 3-59 months (i.e., < 5 years) (Figure 1). LLINs (i.e.,
166 PermaNet 2.0, Olyset, or DawaPlus 2.0) were mass distributed in Bongo District by the National Malaria
167 Elimination Programme (NMEP)/Ghana Health Service (GHS) between 2010-2012 and again in 2016
168 following the discontinuation of IRS (Gogue et al., 2020; Tiedje et al., 2022; US Agency for International
169 Development (USAID) Global Health Supply Chain Program, 2020). In addition, to maintain high coverage
170 of LLINs between these campaigns continuous distribution was undertaken using routine services (i.e.,
171 antenatal clinics, school distributions, immunization visits, etc.) (Tiedje et al., 2022). Over the course of
172 this study self-reported LLIN usage the previous night remained high across all age groups, from 89.1% in
173 2012 (pre-IRS), 83.5% in 2014 (during IRS), 90.6% in 2015 (post-IRS), to 96.8% in 2017 (SMC). Details on
174 the study area, study population, and data collection procedures have been previously described (Tiedje
175 et al., 2022, 2017).
176

177 Details of the IRS and SMC interventions

178 Starting in 2013, the AngloGold Ashanti Malaria Control Programme (AGAMal) in a public-private
179 partnership with the Global Fund, scaled up IRS across all of the Upper East Region of northern Ghana
180 (Gogue et al., 2020). As part of this initiative, three rounds of IRS with organophosphate formulations (i.e.,
181 non-pyrethroid) were rolled out prior to the start of the wet season between 2013 and 2015 (Figure 1A)
182 in Bongo District (Tiedje et al., 2022). Based on AGAMal's operational reports, IRS coverage in Bongo
183 District was 91.8% in Round 1, 95.6% in Round 2, and finally 96.6% in Round 3 (AGAMal, personal

184 communication). To monitor the impact of the IRS on the local vector population, monthly entomological
185 collections were undertaken between February 2013 and September 2015 (Tiedje et al., 2022). Using
186 these surveys, we observed that the monthly entomological inoculation rate (EIR) (infective
187 bites/person/month (ib/p/m)), a measure of local transmission intensity, declined by > 90% at the peak of
188 the wet season between August 2013 (pre-IRS) (EIR = 5.3 ib/p/m) and August 2015 (post-IRS) (EIR = 0.4
189 ib/p/m) (Tiedje et al., 2022). Following the IRS, SMC was rolled out in the Upper East Region by the
190 NMEP/GHS starting in 2016 (Gogue et al., 2020) (Figure 1A). SMC is the intermittent administration of a
191 curative dose of an antimalarial to children between the ages of 3-59 months (i.e., < 5 years) (WHO, 2012).
192 Like other countries, the SMC drug combination of choice in Ghana is sulfadoxine-pyrimethamine plus
193 amodiaquine, which is administered at monthly intervals (i.e., ~28-30 days apart) during the high-
194 transmission season (i.e., wet season) (WHO, 2012). The goal of this age-targeted intervention is to both
195 clear current infections and prevent malarial illness by maintaining a therapeutic concentration of an
196 antimalarial in the blood over the period of greatest risk (i.e., high-transmission season). Reported SMC
197 coverage in Bongo District was 92.6% in 2016 (two cycles between August – September 2016) and 94.6%
198 in 2017 (four cycles between July – October 2017) (Gogue et al., 2020) (NMEP/GHS, personal
199 communication).
200

201 ***Var* genotyping and sequence analysis**

202 Genomic DNA was extracted from the dried blood spots for all participants with a confirmed microscopic
203 asymptomatic *P. falciparum* infection (i.e., isolate) (2,572 isolates, Table supplement 2) using the QIAamp
204 DNA mini kit (QIAGEN, USA) as previously described (Tiedje et al., 2017). For *var* genotyping or *var*coding,
205 the sequence region within the *var* genes encoding the DBLα domains of PfEMP1 were amplified using a

206 single-step PCR, pooled, and sequenced on an Illumina platform using the MiSeq Reagent Kit v3 (600 cycle;
207 2×300bp paired-end) (Supplemental Methods, Figure supplement 1). The raw sequence data was then
208 processed using our previously published customized bioinformatic pipelines (Supplemental Methods,
209 Figure supplement 2). For additional information on the use of these bioinformatic pipelines a detailed
210 tutorial is available (https://github.com/UniMelb-Day-Lab/tutorialDBLalpha).
211
212 DBLα sequencing data was obtained from 2,397 *P. falciparum* isolates (93.2%) (Table supplement 2). This
213 genotyping success was acceptable given that we were working with low-density asymptomatic infections
214 (Table supplement 1). Using a cut-off of ≥ 20 DBLα types, DBLα sequencing data was obtained from 2,099
215 *P. falciparum* isolates (81.6%) with a total of 289,049 DBLα sequences and 53,238 unique DBLα types
216 being identified in the study population (Table supplement 2). The median *P. falciparum* density was ~4
217 times higher for isolates with ≥ 20 DBLα types compared to those that gave no or < 20 DBLα types (520
218 [IQR: 200-1880] parasites/µL vs. 120 [IQR: 40-200] parasites/µL, respectively).
219
220 DBLα type diversity
221 We monitored the impacts of the sequential interventions (i.e., IRS and SMC) on diversity by measuring
222 changes in the population genetics of DBLα types at the population level (i.e., *P. falciparum* reservoir).
223 Diversity was monitored using two measures, DBLα type richness and DBLα type frequency. Richness was
224 defined as the number of unique DBLα types observed (i.e., DBLα type pool size) in each survey or study
225 time point (i.e., 2012, 2014, 2015, and 2017). DBLα type richness, however, does not provide any
226 information about the relative frequencies of the different DBLα types in the population, as they are all
227 weighted equally whether they are observed once or more frequently (e.g., observed in > 20 isolates per

228 survey). To further examine the impacts of the interventions on DBLα type diversity we also assessed the
229 frequency of each unique DBLα type in 2012, 2014, 2015, and 2017. Here we defined DBLα type frequency
230 as the number of times (i.e., number of isolates) a DBLα type was observed in each survey. Both upsA and
231 non-upsA DBLα type diversities were measured due to their different biological features, chromosomal
232 positions (i.e., subtelomeric regions vs. internal or central regions), as well as population genetics (Falk et
233 al., 2009; Gardner et al., 2002; Jensen et al., 2004; Kaestli et al., 2006; Kalmbach et al., 2010; Kraemer et
234 al., 2007; Kraemer and Smith, 2006; Kyriacou et al., 2006; Lavstsen et al., 2003; Normark et al., 2007;
235 Rottmann et al., 2006; Warimwe et al., 2012, 2009; Zhang and Deitsch, 2022). The proportions of upsA
236 and non-upsA *var* genes in a repertoire or single genome have been defined as ~15-20% and ~80-85%,
237 respectively, based on whole genome sequencing (Rask et al., 2010). The upsA and non-upsA DBLα type
238 proportions were partitioned as expected in our analyses, with the median proportions at the repertoire
239 level being comparable in 2012 (19% upsA and 81% non-upsA), 2014 (22% upsA and 78% non-upsA), 2015
240 (21% upsA and 79% non-upsA), and 2017 (20% upsA and 80% non-upsA).
241
242 Repertoire similarity as defined by pairwise type sharing
243 To estimate genetic similarity between the DBLα repertoires (i.e., unique DBLα types identified in each
244 isolate) identified from two isolates, pairwise type sharing (PTS) was calculated between all pairs of
245 isolates in each survey as previously described (Barry et al., 2007). PTS, analogous to the Sørensen Index,
246 is a similarity statistic to evaluate the proportion of DBLα types shared between two isolate repertoires
247 (i.e., DBLα repertoire overlap) and ranges from 0 (i.e., no DBLα repertoire overlap) to 1 (i.e., identical DBLα
248 isolate repertoires), where < 0.50 = unrelated, 0.5 = recent recombinants/siblings, > 0.5 = related, and 1
249 = clones. PTS is a measure of identity-by-state (IBS) used to assess repertoire similarity between isolates

250 and is not used to infer inheritance from a recent common ancestor (i.e., identity-by-decent (IBD)) (Speed
251 and Balding, 2015).
252

253 **DBLα isolate repertoire size**

254 For this study we have exploited the unique population structure of non-overlapping DBLα isolate
255 repertoires to estimate isolate MOI_{var}. To calculate MOI_{var}, the non-upsA DBLα types were chosen since
256 not only are they more diverse and less conserved between isolate repertoires (i.e., low median PTS_{non-}
257 $_{upsA} \leq 0.020$) compared to the upsA DBLα types, but they have also been shown to have a more specific 1-
258 to-1 relationship with a single *var* gene than upsA (Tan et al., 2023). The low to non-existent overlap of
259 repertoires enables an estimation of MOI that relies on the number of non-upsA DBLα types sequenced
260 from an individual's isolate (Ruybal-Pesántez et al., 2022; Tiedje et al., 2022). A constant repertoire size
261 or number of DBLα types in a parasite genome can be used to convert the number of types sequenced in
262 an isolate to estimate MOI (Ruybal-Pesántez et al., 2022; Tiedje et al., 2022). This approach, however,
263 neglects the measurement error in this size introduced by targeted PCR and amplicon sequencing of *var*
264 genes in an isolate.
265

266 **Bayesian estimation of MOI_{var} and associated census population size**

267 Here, we extend the method to a Bayesian formulation and estimate the posterior distribution for each
268 sampled individual for the probability of different MOI values. From individual posterior distributions, we
269 can then obtain the estimated MOI frequency distribution for the population as a whole. The two pieces
270 of information required for our approach are the measurement error and the prior distribution of MOI.
271 The measurement error is simply the repertoire size distribution, that is, the distribution of the number

of non-upsA DBLα types sequenced given MOI = 1, which is empirically available (Figure supplement 3 (Labbé et al., 2023)). We refer to it as P(s | MOI = 1) where *s* here denotes repertoire size. More generally when MOI ≥ 1, *s* denotes the number of non-upsA DBLα types sequenced or isolate size. The prior distribution of MOI refers to the belief we have for what the actual MOI distribution might look like at the population level before empirical evidence is taken into consideration. For example, the prior distribution of MOI is likely to centre around a higher value in high-transmission endemic areas than in low-transmission ones.

We can obtain P(s | MOI = m) from the serial convolution of the repertoire size distribution P(s | MOI = 1) and P(s | MOI = m - 1). Starting with the repertoire size distribution given a single infection, we can derive P(s | MOI = m) for *m* equal to 2,3,..., up until a maximum value of 20 (empirically determined), as follows:

$$P(s \mid MOI = m) = \sum_{x=L}^{U} P(x \mid MOI = 1) \times P(s - x \mid MOI = m - 1) \qquad 1.1$$

where *L* and *U* are the lower and upper limit for the repertoire size, 10 and 45 respectively from the empirical repertoire size distribution (Figure supplement 3 (Labbé et al., 2023)).

For simplicity, we begin with a uniform prior. We use Bayes' rule to derive a posterior distribution of MOI given a certain number of non-upsA DBLα types sequenced from an individual:

$$P(MOI = j \mid s) = \frac{P(s \mid MOI = j) \times P(MOI = j)}{\sum_{i=1}^{k} P(s \mid MOI = i) \times P(MOI = i)} \qquad 1.2$$

291 where *k* is the maximum value of MOI, here 20, as empirically determined.

292

293 To obtain the MOI distribution at the population level, we could either simply pool the maximum *a*
294 *posteriori* MOI estimate for each sampled individual, or use a technique called mixture distribution. For
295 the latter, we weighed each posterior MOI distribution for each sampled individual equally and sum over
296 all posterior distributions at the individual level to derive the MOI distribution at the population level:

297 $$f(MOI = m) = \sum_{i=1}^{n} \frac{1}{n} P(MOI = m \mid s_i) \qquad 1.3$$

298 where *n* is the number of sampled individuals. These two approaches gave similar results for our empirical
299 survey data as determined by the Kolmogorov-Smirnov Test. The obtained distance statistic is close to 0
300 and the corresponding *p-value* is non-significant across all surveys, indicating that the two estimates were
301 drawn from the same distribution (Table supplements 3 and 4). Additionally, the difference between the
302 mean MOI values at the population level obtained from the two approaches is small (Table supplements
303 3 and 4). Given this similarity, we present the results based on pooling the maximum *a posteriori* MOI
304 estimates for each sampled individual in the main text and include the results based on mixture
305 distribution in the Supplemental Information. Note that we focused on individuals who had confirmed
306 microscopic asymptomatic P. *falciparum* infections for our MOI estimation.

307

308 To examine alternative priors, we considered empirical MOI distributions described in the literature
309 including the Poisson, hyper-Poisson, and negative binomial distributions (Dietz, 1988; Henry, 2020). The
310 hyper-Poisson and negative binomial distributions can capture the overdispersion seen in the empirical
311 distribution of MOI for certain areas and caused by factors such as heterogeneous biting. We therefore

312 focused on a negative binomial distribution and investigated changing its parameters to generate priors
313 with different means spanning a wide range of MOI values (mean MOI within [~1.5, ~6.7]), including those
314 seen in high-transmission endemic areas. A uniform prior and a zero-truncated negative binomial
315 distribution with parameters within the range typical of high-transmission endemic regions (higher mean
316 MOI, for example, ~4.3 versus ~6.7, with tails for higher MOI values in the range of 10-20) produce similar
317 MOI estimates at the population level (Table supplements 5 and 6). However, when setting the parameter
318 range of the zero-truncated negative binomial to be representative of those in low-transmission endemic
319 regions where the empirical MOI distribution centres around monoclonal infections with the majority of
320 MOIs = 1 or 2 (mean MOI ≈ 1.5, no tail at higher MOI values), the final population-level MOI distribution
321 does deviate more from that based on the aforementioned prior and parameter choices (Table
322 supplement 6). The final individual- and population-level MOI estimates are not sensitive to the specifics
323 of the prior MOI distribution as long as this distribution captures the tail for higher MOI values with above-
324 zero probability. The obtained Kolmogorov-Smirnov Test distance statistics and their corresponding *p-*
325 *values*, the Pearson correlation tests and their corresponding *p-values*, as well as the difference in mean
326 MOI values, for the comparison of the MOI estimates obtained with the different priors are included in
327 Table supplements 5 and 6. Given these comparisons, we provide in our analyses the estimated
328 population MOI distribution using a uniform prior.
329

330 **Adjusting for differences in sampling depth across age groups and surveys in the census population**
331 **size calculation**

332 In our interrupted time-series study design, we sampled the Bongo population by age group to assess age-
333 specific effects of the sequential interventions (i.e., IRS and SMC). Sampling depth by age group was

334 consistent across the four cross-sectional surveys (Table supplement 1), except for 1-5-years-olds in 2014.
335 To account for variation in sampling depth across age groups and surveys, we performed subsampling at
336 the level of the minimum number of individuals in each age group across all surveys. We calculated the
337 total number of *var* repertoires from a subsample of this number of individuals within each age group for
338 each survey. This approach ensures consistent sample sizes within each age group across all surveys. We
339 summed the *var* repertoires across age groups to obtain the total *var* repertoire count for each survey.
340 To calculate the mean and 95% CIs for the number of *var* repertoires (i.e., census population size), we
341 repeated the subsampling procedure 10,000 times and derived these quantities from the distribution of
342 these repeated subsampling replicates.
343

344 Statistical analysis

345 We used the R v4.3.1 for all data analyses with the collection of R packages in *tidyverse* being used for
346 data curation along with *base*, *stats, gtsummary,* and *epiR* for the statistical analyses (R Core Team, 2018;
347 Sjoberg, D et al., 2021; Stevenson, 2020; Wickham et al., 2019). Continuous variables are presented as
348 medians with interquartile ranges (IQRs) and discrete variables are presented using the observed or
349 calculated values with the 95% confidence interval (95% CIs) or ± 2 standard deviations (± 2SD). Kaplan-
350 Meier survival curves were generated for the time (i.e., number of surveys) to first event (i.e., when the
351 DBLα type was no longer observed/detected) comparing the upsA and non-upsA DBLα types; *p-values*
352 were determined using the log-rank test using the R packages *survival* and *survminer* (Kassambara et al.,
353 2021; Therneau, 2023). The time interval to first event considered for all survival curves was the number
354 of surveys or year (i.e., 2012, 2014, 2015, and 2017) that each DBLα type was observed and only includes

355 those upsA (N = 2,218) and non-upsA (N = 33,159) DBLα types that were seen at baseline in 2012 (i.e.,

356 those DBLα types observed prior to the IRS intervention) (Table supplement 2).

357

358 # RESULTS

359 Between 2013 and 2015, three-rounds of IRS with non-pyrethroid insecticides were implemented across
360 all of Bongo District. Coincident with the > 90% decrease in transmission following IRS (Tiedje et al., 2022),
361 the prevalence of microscopic *P. falciparum* infections compared to the 2012 baseline survey (pre-IRS)
362 declined by 45.2% and 35.7% following the second (2012 to 2014) and the third (2012 to 2015) round of
363 IRS, respectively (Figure 1B, Table supplement 1). These declines in parasite prevalence were observed
364 across all ages, with the greatest impacts being observed on the younger children (1-5 years) who were
365 ~3 times less likely to have an infection in 2015 (post-IRS) compared to 2012 (pre-IRS) (Figure 1C, Table
366 supplement 1). These reductions were however short-lived and in 2017, 32-months after the
367 discontinuation of IRS, but during SMC, overall *P. falciparum* prevalence rebounded to 41.2%, or near pre-
368 IRS levels (Figure 1B, Table supplement 1). Importantly, this increase in the prevalence of infection in 2017
369 was only observed among the older age groups (i.e., ≥ 6 years) (Figure 1C, Table supplement 1). This
370 difference by age group in 2017 can be attributed to SMC, which only targets children between 3-59
371 months (i.e., < 5 years). A notable increase in parasite prevalence for adolescents (11-20 years) and adults
372 (> 20 years) was found in 2017 relative to the 2012 (pre-IRS) (Figure 1C, Table supplement 1).

373

374 Next, we wanted to explore changes in population size measured by MOI_{var}. As this metric is based on
375 non-overlap of *var* repertoire diversity of individual isolates, specifically non-upsA DBLα types, we
376 investigated whether DBLα isolate repertoire similarity (or overlap), as measured by PTS, increased
377 following the sequential interventions (i.e., IRS and SMC). Figure 2 shows that median PTS values for both
378 upsA and non-upsA DBLα types remained low in all surveys, although the PTS distributions for both groups
379 changed significantly at each of the study time points relative to the 2012 baseline survey (pre-IRS) (*p*-

380 *values* < 0.001, Kruskal-Wallis test) (Figure 2). Somewhat unexpectedly, the change was in the direction
381 of reduced similarity (i.e., less overlap) with lower median PTS scores and a larger number of isolates
382 sharing no DBLα types (i.e., PTS = 0) in 2014, 2015, and 2017 compared to 2012. Relevant to measurement
383 of MOI_{var}, the median PTS scores for non-upsA DBLα types were lower following the IRS intervention
384 ($PTS_{non\text{-}upsA}$: 2014 = 0.013 and 2015 = 0.013 vs. $PTS_{non\text{-}upsA}$: 2012 = 0.020). In 2017, the non-upsA PTS
385 distributions shifted back towards higher median PTS scores ($PTS_{non\text{-}upsA}$ = 0.016) and fewer isolates shared
386 no DBLα types relative to 2014 and 2015 (Figure 2). To verify this pattern was not influenced by multiclonal
387 infections (MOI_{var} > 1) we also examined isolates with monoclonal infections (MOI_{var} = 1) and found that
388 this non-overlapping structure persisted regardless of infection complexity, particularly for the non-upsA
389 DBLα types (Figure supplement 4). These PTS data make clear that we were dealing with a large, highly
390 diverse parasite population where 99.9% of the isolate comparisons in all surveys had $PTS_{non\text{-}upsA}$ scores ≤
391 0.1 (i.e., shared ≤ 10% of their non-upsA DBLα types), indicating that DBLα isolate repertoires were highly
392 unrelated (Figure 2). In fact, throughout the IRS, SMC, and subsequent rebound, very few DBLα isolate
393 repertoires were observed to be related, with < 0.003% isolate comparisons in each survey having a $PTS_{non\text{-}upsA}$ ≥ 0.5 (i.e., siblings or recent recombinants) (Figure 2).
394
395
396 The raw data of non-upsA DBLα isolate repertoire sizes (Figure supplement 5) were used to estimate
397 MOI_{var} as adjusted using the Bayesian approach based on pooling the maximum *a posteriori* MOI estimates
398 (Figure 3) and the mixture distribution (Figure supplement 6). We observed that at baseline in 2012, the
399 majority (89.2%) of the population across all ages carried multiclonal infections (median MOI_{var} = 4 [IQR:
400 2 – 6]) (Figure 3A). Following the IRS intervention, the estimated MOI_{var} distributions became more
401 positively skewed, indicating that a lower proportion of participants harboured multiclonal infections with

402 a lower median MOI_{var} in 2014 (64.5%; median MOI_{var} = 2 [IQR: 1 – 3]) and 2015 (71.4%; median MOI_{var} =
403 2 [IQR: 1 – 3]) compared to 2012 (Figure 3A). These reductions in median MOI_{var} and the proportion of
404 multiclonal infections, which were observed across all age groups (Figure 3B), are consistent with the >
405 90% decrease in transmission intensity following the IRS in turn reducing exposure to new parasite
406 genomes. However, in 2017, both median MOI_{var} (3 [IQR: 2 – 4]) and the proportion of multiclonal
407 infections (78.9%) rebounded in all age groups, even among the younger children (1-5 years)
408 predominantly targeted by SMC (Figure 3). While the prevalence of infection in 2017 remained low for
409 the younger children (1-5 years), those infected still carried multiclonal infections (84.1% of those
410 infected) (Figure 3B). Although the MOI_{var} distributions across all age groups started to rebound in 2017
411 (i.e., less positively skewed compared to 2014 and 2015) they had not fully recovered to the 2012 baseline
412 patterns (Figure 3). This was most apparent among the younger children (1-5 years), as a larger proportion
413 of isolates in 2017, compared to 2012, had MOI_{var} values equal to one or two, while a smaller proportion
414 had MOI_{var} values ≥ 5 (Figure 3B).
415
416 Census population size, measured as the number of *P. falciparum var* repertoires circulating in the
417 population during each survey, was estimated by summation of isolate MOI_{var} (see Materials and
418 Methods; Figure 4, Table supplement 7). In 2014 during IRS, this number decreased by 71.4% relative to
419 the 2012 baseline survey (pre-IRS) (Figure 4CE), whereas prevalence decreased by 54.5% (Figure 4CE).
420 Although census population size increased slightly in 2015 relative to 2014 (Figure 4A), there were still
421 64.4% fewer *var* repertoires in the population compared to 2012 (Figure 4CE) in comparison to a 42.6%
422 decrease in prevalence (Figure 4CE). Importantly this loss of *var* repertoires in 2014 and 2015 following
423 the IRS intervention was seen for all age groups (Figure 4B), with the greatest overall reductions (≥ 83.8%)

424 being observed for the younger children (1-5 years) (Figure 4DF). However, in 2017, the number of diverse
425 *var* repertoires in the population rebounded, more than doubling between 2015 and 2017 (Figure 4CE).
426 This increase in the number of *var* repertoires was seen for all age groups in 2017, except for the younger
427 children (1-5 years) where those up to 59 months were targeted by SMC (Figure 4BD). In fact, the greatest
428 overall increase was observed for the adolescents (11-20 years) and adults (> 20 years), where the number
429 of *var* repertoires in 2017 was ~1.2 times higher compared to 2012 (Figure 4F). Similar trends in the
430 number *var* repertoires were also observed for the older children (6-10 years) in 2017, although the
431 rebound was not as striking as that detected for the adolescents and adults.
432
433 As census population size changed considerably during the sequential IRS and SMC interventions, we
434 investigated how the removal or loss of *P. falciparum var* repertoires and subsequent rebound in 2017
435 altered DBLα type richness, measured as the number of unique upsA and non-upsA DBLα types in the
436 parasite population in each survey. Richness at baseline in 2012 (pre-IRS) was high with a large number of
437 unique DBLα types (upsA = 2,218; non-upsA = 33,159) (Figure 5, Table supplement 2) and limited overlap
438 of *var* repertoires (i.e., median $PTS_{non\text{-}upsA} \leq 0.020$) seen in a relatively small study population of 685
439 microscopically positive individuals (Figure 2). In 2014, as *P. falciparum* prevalence and census population
440 size declined (Figure 4) so too did the number of DBLα types, resulting in a 32.2% and 55.3% reduction in
441 richness for the upsA and non-upsA DBLα types, respectively, compared to 2012 (Figure 5, Table
442 supplement 2). Again in 2015, as *P. falciparum* prevalence and population size remained low (Figure 4)
443 DBLα type richness was still less than that observed in 2012 (24.6% and 46.0% reduction for upsA and
444 non-upsA DBLα types, respectively) (Figure 5, Table supplement 2). Finally, in 2017, we found that upsA

445 and non-upsA DBLα type richness rebounded relative to 2014 and 2015, coincident with the increase in
446 *P. falciparum* prevalence and census population size (Figure 4, Figure 5).
447
448 Given this reduction in DBLα type richness following the IRS intervention and subsequent rebound in 2017,
449 we wanted to explore whether the loss of richness was influenced by the frequency of individual DBLα
450 types in the parasite population within and among surveys. To answer this, we defined the relative
451 frequency of individual DBLα types in all isolates in each survey (Figure 6, Figure supplement 7). We
452 discovered that individual upsA and non-upsA DBLα types were not all at equal frequencies within a survey
453 and among surveys. They could be classified as frequent (i.e., observed in 11-20 or > 20 isolates), less
454 frequent (i.e., observed in 2-10 isolates) or only seen once, at baseline in 2012 (Figure 6AB). In 2014 and
455 2015, following IRS, there was a significant increase in the proportion of upsA and non-upsA DBLα types
456 in the lower frequency categories (*p-value* < 0.001, Mann-Whitney U test), with all DBLα types becoming
457 rarer in the population (Figure 6CD). This change can be attributed to the removal of *P. falciparum var*
458 repertoires (Figure 4) with associated loss of upsA and non-upsA DBLα type richness (Figure 5), which
459 disproportionally affected those DBLα types seen once. This shift to all DBLα types becoming rarer
460 following IRS changed in 2017, where the proportion of DBLα types in the more frequent categories (i.e.,
461 2-10, 11-20, or > 20 isolates) significantly increased while the proportion seen once decreased (*p-values*
462 < 0.001, Mann-Whitney U tests) (Figure 6CD). Data in Figure 6 (A-D) pointed to a differential effect of the
463 IRS intervention and subsequent rebound on the less frequent upsA and non-upsA DBLα types vs. those
464 that were classified as frequent, where those DBLα types that were most frequent persisted longitudinally.
465

466 To explore this observation further we restricted the longitudinal analysis to those DBLα types from the
467 baseline survey in 2012 (pre-IRS). We compared the probability of survival for the DBLα types identified
468 at baseline in 2012 and found that the upsA DBLα types persisted significantly longer in the population
469 relative to the non-upsA DBLα types ($p < 0.001$, log-rank test), despite the IRS intervention. The simple
470 explanation being that although the upsA DBLα types had lower richness (Figure 5), a larger proportion
471 was classified as frequent indicating that multiple copies existed in the population compared to the non-
472 upsA DBLα types (Figure 6CD). Furthermore, when we examined survival using the frequency categories,
473 the upsA and non-upsA DBLα types that were observed at multiple study time points (i.e., 2012, 2014,
474 2015, and 2017), albeit in different isolate repertoires, were those that were most frequent (i.e., observed
475 in 11-20 and >20 isolates) in the population at baseline in 2012 (Figure 6EF). As expected, the DBLα types
476 that were only observed once in 2012, were significantly less likely to be seen longitudinally (*p-value* <
477 0.001, log-rank test) (Figure 6EF). These differential changes in DBLα type richness with respect to rare vs.
478 frequent DBLα types are a consequence of changes in census population size with interventions (Figure
479 4) where each isolate repertoire is composed of many rare DBLα types as defined by PTS (Figure 2).
480

481 # DISCUSSION

482 *P. falciparum* populations in high-transmission endemic areas in SSA, are characterised by extensive
483 diversity, high rates of recombination, as well as frequent multiclonal infections. Here we defined census
484 population size of *P. falciparum* to understand total parasite diversity in a human population and explore
485 the age-specific efficacy of malaria interventions to reduce this metric in such areas as typified by Bongo,
486 Ghana. Census population size proved more informative than parasite prevalence alone because it
487 captures "within" host parasite population size as MOI, rather than using the infected host per se as a unit
488 of population size. Whilst the concept of census population size is agnostic of how you measure MOI, the
489 extensive DBLα isolate repertoire diversity presented makes a strong case for fingerprinting parasite
490 isolates by *var*coding in high transmission. This is opposed to looking at allelic diversity of a single copy
491 antigen gene, such as *csp*.

492

493 Census population size is a total enumeration or count of infections in a given population sample and over
494 a given time period in an ecological sense, distinct from the formal effective population size (N_e) used in
495 population genetics (Charlesworth, 2009). Given the low overlap between *var* repertoires of parasites
496 observed in monoclonal infections (MOI = 1), the census population size calculated in Bongo, Ghana
497 translates to a diversity of strains or repertoires. The distinction of census population size in terms of
498 infection counts and effective population size from population genetics has been made before for
499 pathogens, including the seasonal influenza virus and the measles virus (Bedford et al., 2011); it is also a
500 distinction made in the ecological literature for non-pathogen populations (Palstra and Fraser, 2012). The
501 census population size of a given population sample depends of course on sample size and was used here
502 for comparisons across time of samples of the same depth (i.e., ~2,000 individuals). There is, however, a

503 simple map between census population size and mean MOI, as one can simply divide or multiply by the
504 sample size, respectively, to convert between the two quantities (Table supplement 7). Therefore, one
505 can extrapolate from the census population size of a given population sample to that of the whole
506 population of local hosts in a given area to compare across studies that differ in sampling depth and/or
507 spatial extent. What is needed for this extrapolation is a stable mean MOI relative to the sample size or
508 sampling depth, which is indeed the case in this study (Figure supplement 8) and can be easily checked in
509 other studies. Given the typical duration of infection, we expect our population size to be representative
510 of a per-generation measure.
511
512 By *var*coding we identified a very large census parasite population size in a relatively small human
513 population of ~2,000 individuals at baseline and captured age-specific changes in this metric in response
514 to sequential malaria control interventions. IRS reduced the MOI_{var} parasite population size substantially
515 with the greatest reductions (85%) seen in the younger children (1-5 years). More than two years after
516 cessation of IRS, rebound in 2017 was rapid in all age groups, except for the younger children (1-5 years)
517 where those up to 59 months were targeted by SMC. Population sizes in adolescents (11-20 years) and
518 adults (> 20 years) showed they carried more infections in 2017 than at baseline in 2012. This is indicative
519 of a loss of immunity during IRS which may relate to the observed loss of *var* richness, especially the many
520 rare types. This warrants further investigation of changes in variant-specific immunity. During and
521 following the IRS and SMC interventions, *var* diversity remained high and *var* repertoire overlap remained
522 low, reflecting characteristic properties of high transmission and demonstrating the overall resilience of
523 the species to survive significant short-term perturbations. Combining interventions and targeting older

524 age groups or the whole community with chemoprevention would no doubt have a much greater impact
525 on reducing the diversity of the reservoir of infection.
526
527 What was striking about the Bongo study was the speed with which rebound in MOI_{var} per person and
528 census population size occurred, once the short-term IRS was discontinued. We looked for a potential
529 explanation in our genetic data. PTS and population frequency data showed that many of the DBLα types
530 occurred in multiple repertoires or genomes. This enabled the survival of these more frequent DBLα types
531 through the interventions, facilitating rebound by maintenance of this diversity. The other notable
532 population genetic result of our study was the failure to increase similarity (or relatedness by state) of *var*
533 repertoires by reducing transmission by > 90% via IRS. From a baseline of a very large population size with
534 very low overlap in repertoires you need outcrossing to create relatedness. However, this was less likely
535 to happen due to reduced transmission as a result of IRS. Rebound, with associated increases in
536 transmission, led to a small increase in *var* repertoire similarity. This is the opposite to what has been
537 observed in areas of lower transmission under intense malaria control where the intensity of interventions
538 led to increased genome similarity, as assessed by IBD, from a starting point of much lower genome
539 diversity and greater relatedness (Daniels et al., 2015).
540
541 Our molecular approach to measure population size has been to sum MOI_{var} in individual hosts with
542 microscopically-detectable infections. Like any diagnostic method there are limits to sensitivity and
543 specificity, which can be more or less tolerated dependent upon the purpose of the study. Here we have
544 looked at relative changes in population size with sequential interventions using an interrupted time-
545 series study design and observed changes by measuring MOI_{var}. We have accounted for missing DBLα type

546 data where complete *var* repertoires may not have been sequenced using a Bayesian method based on
547 empirical knowledge of the measurement error. This approach has conceptual relation to the Bayesian
548 approach by Johnson and Larremore (Johnson and Larremore, 2022) to estimate complete repertoire size
549 of, and overlap between, monoclonal infections from incomplete sampling of DBLα types. Our
550 measurement of population size based on MOI_{var} will be subject to other sampling errors which may in
551 the end be more significant (discussed in detail in Labbé et al. (Labbé et al., 2023)). For example, low
552 parasitemia typical of asymptomatic infections, small blood volumes, clinical status, and/or within host
553 dynamics, including synchronicity, will all create sampling problems, but these are common to all
554 measures of MOI.
555
556 Previously, we have drawn attention to the potential underestimation of the number of DBLα types of
557 related parasites generated by a cross, when using *var* genotyping (Labbé et al., 2023). Such related
558 parasites must be created frequently in high transmission due to extensive outcrossing (Babiker et al.,
559 1994; Paul et al., 1995). Single clone genomics experiments using biallelic SNPs from whole genome
560 sequencing data have also detected related parasites using IBD in clinical infections from humans in a
561 high-transmission area of Malawi (Nkhoma et al., 2020). Here we have analysed low- to moderate-density,
562 chronic, asymptomatic infections (see Table supplement 1) under strong immune selection in semi-
563 immune hosts whom we have shown select against parasites with high PTS scores consistent with
564 relatedness by decent (Day et al., 2017; He et al., 2018; Ruybal-Pesántez et al., 2022). When considering
565 the importance of possible exclusion of parasites related by descent, the only sure way to detect such
566 parasites in high transmission is by single cell genomics, a methodology of limited application to malaria

surveillance due to practicality and cost of scale up. Again, the error from failure to sample infections related by descent must be weighed up against the issues of under-sampling as described above.

The Bayesian approach of the *var*coding method relies on the low or limiting similarity of *var* repertoires infecting individual human hosts. As such, it would appear to break down as the *var* repertoire overlap moves away from extremely low, and therefore, for locations with lower transmission intensity. Interestingly, this is not the case in the numerical simulations of Labbé et al. (Labbé et al., 2023), for a gradient of three transmission intensities, from high to low, with the original *var*coding method performing well across the gradient. This robustness of the method may arise from a nonlinear and fast transition from low to high overlap that is accompanied by MOI changing rapidly from primarily multiclonal (MOI > 1) to monoclonal (MOI = 1) infections. This matter needs to be investigated further in the future, including ways to extend the Bayesian approach to explicitly include the distribution of *var* repertoire overlap.

In summary, our findings provide parasite population insights into why rebound is the inevitable consequence of such short-term IRS interventions unless you simultaneously target the highly diverse, long-lived parasite population in humans, not just children < 5 years by SMC. Of potential translational significance for malaria molecular surveillance, we identify new metrics, especially MOI_{var} and census population size as well as *var* frequency category, informative to monitor and evaluate interventions in high-transmission areas with multiclonal infections and high rates of outcrossing. Such metrics could be used longitudinally to detect incremental gains of transmission-reducing interventions, including IRS,

588 LLINs, and vaccines to perturb the high-transmission characteristics of the parasite population in humans

589 in high-burden countries in SSA.

590

591 ACKNOWLEDGMENTS. This research was supported by Fogarty International Center at the National
592 Institutes of Health through the joint NIH-NSF-NIFA Ecology and Evolution of Infectious Diseases award
593 R01-TW009670 to K.A.K, M.P, and K.P.D; and the National Institute of Allergy and Infectious Diseases,
594 National Institutes of Health through the joint NIH-NSF-NIFA Ecology and Evolution of Infectious Diseases
595 award R01-AI149779 to A.R.O, K.A.K, M.P, and K.P.D. We wish to thank the participants, communities, and
596 the Ghana Health Service in Bongo District, Ghana for their willingness to participate in this study. We
597 would like to thank the field teams in Bongo for their technical assistance in the field, as well as the
598 laboratory personnel at the Navrongo Health Research Centre for their expertise and for undertaking the
599 sample collections and parasitological assessments.

600

REFERENCES

Anderson TJC, Haubold B, Williams JT, Estrada-Franco JG, Richardson L, Mollinedo R, Bockarie M, Mokili J, Mharakurwa S, French N, Whitworth J, Velez ID, Brockman AH, Nosten F, Ferreira MU, Day KP, Estrada-Franco JG, Richardson L, Mollinedo R, Bockarie M, Mokili J, Mharakurwa S, French N, Whitworth J, Velez ID, Brockman AH, Nosten F, Ferreira MU, Day KP. 2000. Microsatellite markers reveal a spectrum of population structures in the malaria parasite Plasmodium falciparum. *Mol Biol Evol* **17**:1467–1482. doi:10.1093/oxfordjournals.molbev.a026247

Babiker HA, Ranford-Cartwright LC, Currie D, Charlwood JD, Billingsley P, Teuscher T, Walliker D. 1994. Random mating in a natural population of the malaria parasite Plasmodium falciparum. *Parasitology* **109**:413–421. doi:10.1017/S0031182000080665

Barry AE, Leliwa-Sytek A, Tavul L, Imrie H, Migot-Nabias F, Brown SM, McVean GA V, Day KP. 2007. Population genomics of the immune evasion (var) genes of Plasmodium falciparum. *PLoS Pathog* **3**:e34. doi:10.1371/journal.ppat.0030034

Bedford T, Cobey S, Pascual M. 2011. Strength and tempo of selection revealed in viral gene genealogies. *BMC Evol Biol* **11**. doi:10.1186/1471-2148-11-220

Bruce MC, Galinski MR, Barnwell JW, Donnelly CA, Walmsley M, Alpers MP, Walliker D, Day KP. 2000. Genetic diversity and dynamics of plasmodium falciparum and P. vivax populations in multiply infected children with asymptomatic malaria infections in Papua New Guinea. *Parasitology* **121 (Pt 3**:257–272. doi:10.1017/S0031182099006356

Charlesworth B. 2009. Fundamental concepts in genetics: Effective population size and patterns of molecular evolution and variation. *Nat Rev Genet*. doi:10.1038/nrg2526

Chen DS, Barry AE, Leliwa-Sytek A, Smith T-AA, Peterson I, Brown SM, Migot-Nabias F, Deloron P, Kortok MM, Marsh K, Daily JP, Ndiaye D, Sarr O, Mboup S, Day KP. 2011. A molecular epidemiological study of var gene diversity to characterize the reservoir of Plasmodium falciparum in humans in Africa. *PLoS One* **6**:e16629. doi:10.1371/journal.pone.0016629

Daniels RF, Schaffner SF, Wenger E a., Proctor JL, Chang H-H, Wong W, Baro N, Ndiaye D, Fall FB, Ndiop M, Ba M, Milner D a., Taylor TE, Neafsey DE, Volkman SK, Eckhoff P a., Hartl DL, Wirth DF. 2015. Modeling malaria genomics reveals transmission decline and rebound in Senegal. *PNAS* **112**:7067–7072. doi:10.1073/pnas.1505691112

Day KP, Artzy-Randrup Y, Tiedje KE, Rougeron V, Chen DS, Rask TS, Rorick MM, Migot-Nabias F, Deloron P, Luty AJF, Pascual M. 2017. Evidence of Strain Structure in Plasmodium falciparum Var Gene Repertoires in Children from Gabon, West Africa. *PNAS* **114**:E4103–E4111. doi:10.1073/pnas.1613018114

Dietz K. 1988. Mathematical models for transmission and control of malariaMalaria: Principles and Practice of Malariology.

Falk N, Kaestli M, Qi W, Ott M, Baea K, Cortés A, Beck H-P. 2009. Analysis of Plasmodium falciparum var genes expressed in children from Papua New Guinea. *Journal of infectious diseases* **200**:347–356. doi:10.1086/600071

Falk N, Maire N, Sama W, Owusu-Agyei S, Smith T, Beck HP, Felger I. 2006. Comparison of PCR-RFLP and genescan-based genotyping for analyzing infection dynamics of Plasmodium falciparum. *American Journal of Tropical Medicine and Hygiene* **74**:944–950.

642 Farnert A, Snounou G, Rooth I, Bjorkman A. 1997. Daily dynamics of Plasmodium falciparum
643 subpopulations in asymptomatic children in a holoendemic area. *American Journal of Tropical*
644 *Medicine and Hygiene* **56**:538–547. doi:10.4269/ajtmh.1997.56.538
645 Futse JE, Brayton KA, Dark MJ, Knowles DP, Palmer GH. 2008. Superinfection as a driver of genomic
646 diversification in antigenically variant pathogens. *Proc Natl Acad Sci U S A* **105**:2123–2127.
647 doi:10.1073/pnas.0710333105
648 Gardner MJ, Hall N, Fung E, White O, Berriman M, Hyman RW, Carlton JM, Pain A, Nelson KE, Bowman S,
649 Paulsen IT, James K, Eisen J a, Rutherford K, Salzberg SL, Craig A, Kyes S, Chan M-S, Nene V, Shallom
650 SJ, Suh B, Peterson J, Angiuoli S, Pertea M, Allen J, Selengut J, Haft D, Mather MW, Vaidya AB, Martin
651 DMA, Fairlamb AH, Fraunholz MJ, Roos DS, Ralph S a, McFadden GI, Cummings LM, Subramanian
652 GM, Mungall C, Venter JC, Carucci DJ, Hoffman SL, Newbold C, Davis RW, Fraser CM, Barrell B. 2002.
653 Genome sequence of the human malaria parasite Plasmodium falciparum. *Nature* **419**:498–511.
654 doi:10.1038/nature01097
655 Ghansah A, Tiedje KE, Argyropoulos DC, Onwona CO, Deed SL, Labbé F, Oduro AR, Koram KA, Pascual M,
656 Day KP. 2023. Comparison of molecular surveillance methods to assess changes in the population
657 genetics of Plasmodium falciparum in high transmission. *Frontiers in Parasitology* **2**:1067966.
658 Gogue C, Wagman J, Tynuv K, Saibu A, Yihdego Y, Malm K, Mohamed W, Akplu W, Tagoe T, Ofosu A,
659 Williams I, Asiedu S, Richardson J, Fornadel C, Slutsker L, Robertson M. 2020. An observational
660 analysis of the impact of indoor residual spraying in Northern, Upper East, and Upper West Regions
661 of Ghana: 2014 through 2017. *Malar J* **19**:1–13. doi:10.1186/s12936-020-03318-1
662 He Q, Pilosof S, Tiedje KE, Ruybal-Pesántez S, Artzy-Randrup Y, Baskerville EB, Day KP, Pascual M. 2018.
663 Networks of genetic similarity reveal non-neutral processes shape strain structure in Plasmodium
664 falciparum. *Nat Commun* **9**:1817. doi:10.1038/s41467-018-04219-3
665 Henry JM. 2020. A hybrid model for the effects of treatment and demography on malaria superinfection.
666 *J Theor Biol* **491**:110194.
667 Jensen ATR, Magistrado P, Sharp S, Joergensen L, Lavstsen T, Chiucchiuini A, Salanti A, Vestergaard LS,
668 Lusingu JP, Hermsen R, Sauerwein R, Christensen J, Nielsen MA, Hviid L, Sutherland C, Staalsoe T,
669 Theander TG. 2004. Plasmodium falciparum associated with severe childhood malaria preferentially
670 expresses PfEMP1 encoded by group A var genes. *J Exp Med* **199**:1179–1190.
671 doi:10.1084/jem.20040274
672 Johnson EK, Larremore DB. 2022. Bayesian estimation of community size and overlap from random
673 subsamples. *PLoS Comput Biol* **18**:1–16. doi:10.1371/journal.pcbi.1010451
674 Kaestli M, Cockburn I a, Cortés A, Baea K, Rowe JA, Beck H-P. 2006. Virulence of malaria is associated with
675 differential expression of Plasmodium falciparum var gene subgroups in a case-control study. *J Infect*
676 *Dis* **193**:1567–1574. doi:JID35650 [pii]\n10.1086/503776
677 Kalmbach Y, Rottmann M, Kombila M, Kremsner PG, Beck H-P, Kun JFJ. 2010. Differential var gene
678 expression in children with malaria and antidromic effects on host gene expression. *Journal of*
679 *Infectious Diseases* **202**:313–317. doi:10.1086/653586
680 Kassambara A, Kosinski M, Biecek P, Scheipl F. 2021. survminer: Drawing Survival Curves using ggplot2.
681 Kraemer SM, Kyes SA, Aggarwal G, Springer AL, Nelson SO, Christodoulou Z, Smith LM, Wang W, Levin E,
682 Newbold CI, Myler PJ, Smith JD. 2007. Patterns of gene recombination shape var gene repertoires in
683 Plasmodium falciparum: comparisons of geographically diverse isolates. *BMC Genomics* **8**:45.
684 doi:10.1186/1471-2164-8-45

685 Kraemer SM, Smith JD. 2006. A family affair: var genes, PfEMP1 binding, and malaria disease. *Curr Opin*
686 *Microbiol*. doi:10.1016/j.mib.2006.06.006
687 Kyriacou HM, Stone GN, Challis RJ, Raza A, Lyke KE, Thera MA, Koné AK, Doumbo OK, Plowe C V., Rowe JA.
688 2006. Differential var gene transcription in Plasmodium falciparum isolates from patients with
689 cerebral malaria compared to hyperparasitaemia. *Mol Biochem Parasitol* **150**:211–218.
690 doi:10.1016/j.molbiopara.2006.08.005
691 Labbé F, He Q, Zhan Q, Tiedje KE, Argyropoulos DC, Tan MH, Ghansah A, Day KP, Pascual M. 2023. Neutral
692 vs . non-neutral genetic footprints of Plasmodium falciparum multiclonal infections. *PLoS Comput*
693 *Biol* **19**:e1010816. doi:doi.org/10.1101/2022.06.27.497801
694 LaVerriere E, Schwabl P, Carrasquilla M, Taylor AR, Johnson ZM, Shieh M, Panchal R, Straub TJ, Kuzma R,
695 Watson S, Buckee CO, Andrade CM, Portugal S, Crompton PD, Traore B, Rayner JC, Corredor V, James
696 K, Cox H, Early AM, MacInnis BL, Neafsey DE. 2022. Design and implementation of multiplexed
697 amplicon sequencing panels to serve genomic epidemiology of infectious disease: A malaria case
698 study. *Mol Ecol Resour* 2285–2303. doi:10.1111/1755-0998.13622
699 Lavstsen T, Salanti A, Jensen ATR, Arnot DE, Theander TG. 2003. Sub-grouping of Plasmodium falciparum
700 3D7 var genes based on sequence analysis of coding and non-coding regions. *Malar J* **2**:27.
701 doi:10.1186/1475-2875-2-27
702 Lerch A, Koepfli C, Hofmann NE, Kattenberg JH, Rosanas-Urgell A, Betuela I, Mueller I, Felger I. 2019.
703 Longitudinal tracking and quantification of individual Plasmodium falciparum clones in complex
704 infections. *Sci Rep* **9**:1–8. doi:10.1038/s41598-019-39656-7
705 Lerch A, Koepfli C, Hofmann NE, Messerli C, Wilcox S, Kattenberg JH, Betuela I, O'Connor L, Mueller I,
706 Felger I. 2017. Development of amplicon deep sequencing markers and data analysis pipeline for
707 genotyping multi-clonal malaria infections. *BMC Genomics* **18**:1–13. doi:10.1186/s12864-017-4260-
708 y
709 Markwalter CF, Menya D, Wesolowski A, Esimit D, Lokoel G, Kipkoech J, Freedman E, Sumner KM, Abel L,
710 Ambani G, Meredith HR, Taylor SM, Obala AA, O'Meara WP. 2022. Plasmodium falciparum
711 importation does not sustain malaria transmission in a semi-arid region of Kenya. *PLOS Global Public*
712 *Health* **2**:e0000807. doi:10.1371/journal.pgph.0000807
713 Nelson CS, Sumner KM, Freedman E, Saelens JW, Obala AA, Mangeni JN, Taylor SM, O'Meara WP. 2019.
714 High-resolution micro-epidemiology of parasite spatial and temporal dynamics in a high malaria
715 transmission setting in Kenya. *Nat Commun* **10**. doi:10.1038/s41467-019-13578-4
716 Nkhoma SC, Trevino SG, Gorena KM, Nair S, Khoswe S, Jett C, Garcia R, Daniel B, Dia A, Terlouw DJ, Ward
717 SA, Anderson TJC, Cheeseman IH. 2020. Co-transmission of Related Malaria Parasite Lineages Shapes
718 Within-Host Parasite Diversity. *Cell Host Microbe* **27**:93-103.e4. doi:10.1016/j.chom.2019.12.001
719 Normark J, Nilsson D, Ribacke U, Winter G, Moll K, Wheelock CE, Bayarugaba J, Kironde F, Egwang TG,
720 Chen Q, Andersson B, Wahlgren M. 2007. PfEMP1-DBL1alpha amino acid motifs in severe disease
721 states of Plasmodium falciparum malaria. *Proc Natl Acad Sci U S A* **104**:15835–40.
722 doi:10.1073/pnas.0610485104
723 Otto TD, Assefa SA, Böhme U, Sanders MJ, Kwiatkowski DP, Berriman M, Newbold C. 2019. Evolutionary
724 analysis of the most polymorphic gene family in falciparum malaria. *Wellcome Open Res* **4**:1–29.
725 doi:10.12688/wellcomeopenres.15590.1
726 Palstra FP, Fraser DJ. 2012. Effective/census population size ratio estimation: A compendium and
727 appraisal. *Ecol Evol* **2**:2357–2365. doi:10.1002/ece3.329

Paul RE, Packer MJ, Walmsley M, Lagog M, Ranford-Cartwright LC, Paru R, Day KP. 1995. Mating patterns in malaria parasite populations of Papua New Guinea. *Science (1979)* **269**:1709–1711.

R Core Team. 2018. R: A Language and Environment for Statistical Computing. *R Foundation for Statistical Computing*.

Rask TS, Hansen D, Theander TG, Pedersen AG, Lavstsen T, Gorm Pedersen A, Lavstsen T, Pedersen AG, Lavstsen T, Gorm Pedersen A, Lavstsen T. 2010. Plasmodium falciparum erythrocyte membrane protein 1 diversity in seven genomes - divide and conquer. *PLoS Comput Biol* **6**:e1000933. doi:10.1371/journal.pcbi.1000933

Rottmann M, Lavstsen T, Mugasa JP, Kaestli M, Jensen ATR, Müller D, Theander T, Beck H-PP. 2006. Differential expression of var gene groups is associated with morbidity caused by Plasmodium falciparum infection in Tanzanian children. *Infect Immun* **74**:3904–3911. doi:10.1128/IAI.02073-05

Ruybal-Pesántez S, Tiedje KE, Pilosof S, Tonkin-Hill G, He Q, Rask TS, Amenga-Etego L, Oduro AR, Koram KA, Pascual M, Day KP. 2022. Age-specific patterns of DBLa var diversity can explain why residents of high malaria transmission areas remain susceptible to Plasmodium falciparum blood stage infection throughout life. *Int J Parasitol* **20**:721–731.

Ruybal-Pesántez S, Tiedje KE, Tonkin-Hill G, Rask TS, Kamya MR, Greenhouse B, Dorsey G, Duffy MF, Day KP. 2017. Population genomics of virulence genes of Plasmodium falciparum in clinical isolates from Uganda. *Sci Rep* **7**:11810. doi:10.1038/s41598-017-11814-9

Sjoberg, D, Whiting K, Curry M, Lavery J, Larmarange J. 2021. Reproducible Summary Tables with the gtsummary Package. *R J* **13**:570–580.

Smith T, Felger I, Fraser-Hurt N, Beck H-PP. 1999. Effect of insecticide-treated falciparum infections bed nets on the dynamics of multiple Plasmodium falciparum infections. *Trans R Soc Trop Med Hyg* **93 (Supp)**:S1/53-S1/57. doi:10.1016/S0035-9203(99)90328-0

Speed D, Balding DJ. 2015. Relatedness in the post-genomic era: Is it still useful? *Nat Rev Genet* **16**:33–44. doi:10.1038/nrg3821

Stevenson M. 2020. epiR: Tools for the analysis of epidemiological data.

Sumner KM, Freedman E, Abel L, Obala A, Pence BW, Wesolowski A, Meshnick SR, Prudhomme-O'Meara W, Taylor SM. 2021. Genotyping cognate Plasmodium falciparum in humans and mosquitoes to estimate onward transmission of asymptomatic infections. *Nat Commun* **12**:1–12. doi:10.1038/s41467-021-21269-2

Tan MH, Shim H, Chan Y, Day KP. 2023. Unravelling chaos for malaria surveillance : Relationship between DBLα types and var genes in Plasmodium falciparum. *Frontiers in Parasitology* **1**. doi:https://doi.org/10.3389/fpara.2022.1006341

Tessema SK, Hathaway NJ, Teyssier NB, Murphy M, Chen A, Aydemir O, Duarte EM, Simone W, Colborn J, Saute F, Crawford E, Aide P, Bailey JA, Greenhouse B. 2020. Sensitive, highly multiplexed sequencing of microhaplotypes from the Plasmodium falciparum heterozygome. *Journal of Infectious Diseases* **225**:1227–1237.

Therneau T. 2023. A Package for Survival Analysis in R.

Tiedje KE, Oduro AR, Agongo G, Anyorigiya T, Azongo D, Awine T, Ghansah A, Pascual M, Koram KA, Day KP. 2017. Seasonal Variation in the Epidemiology of Asymptomatic Plasmodium falciparum Infections Across Two Catchment Areas in Bongo District, Ghana. *Am J Trop Med Hyg* **97**:199–212. doi:10.4269/ajtmh.16-0959

Tiedje KE, Oduro AR, Bangre O, Amenga-Etego L, Dadzie SK, Appawu MA, Frempong K, Asoala V, Charles A Narh, Samantha L Deed, Ruybal-Pesántez S, Argyropoulos DC, Anita Ghansah, Agyei SA, Segbaya S,

Desewu K, Williams I, Simpson JA, Malm K, Pascual M, Koram KA, Day KP. 2022. Indoor residual spraying with a non-pyrethroid insecticide reduces the reservoir of Plasmodium falciparum in a high-transmission area in northern Ghana. *PLOS Global Public Health* **2**:e0000285. doi:10.1371/journal.pgph.0000285

US Agency for International Development (USAID) Global Health Supply Chain Program. 2020. Technical Breif: Data visability makes all the difference in Ghana's 2018 LLIN mass distribution campaign.

US President's Malaria Initiative Africa IRS (AIRS) Project. 2016. Entomological monitoring of the PMI AIRS program in northern Ghana: 2016 annual report. Bethesda, Marland, USA.

Wagman J, Gogue C, Tynuv K, Mihigo J, Bankineza E, Bah M, Diallo D, Saibu A, Richardson JH, Kone D, Fomba S, Bernson J, Steketee R, Slutsker L, Robertson M. 2018. An observational analysis of the impact of indoor residual spraying with non-pyrethroid insecticides on the incidence of malaria in Ségou Region, Mali: 2012–2015. *Malar J* **17**:19. doi:10.1186/s12936-017-2168-2

Warimwe GM, Fegan G, Musyoki JN, Newton CRJC, Opiyo M, Githinji G, Andisi C, Menza F, Kitsao B, Marsh K, Bull PC. 2012. Prognostic indicators of life-threatening malaria are associated with distinct parasite variant antigen profiles. *Sci Transl Med* **4**:129ra45. doi:10.1126/scitranslmed.3003247

Warimwe GM, Keane TM, Fegan G, Musyoki JN, Newton CRJC, Pain A, Berriman M, Marsh K, Bull PC. 2009. Plasmodium falciparum var gene expression is modified by host immunity. *Proc Natl Acad Sci U S A* **106**:21801–21806.

Watson OJ, Okell LC, Hellewell J, Slater HC, Unwin HJT, Omedo I, Bejon P, Snow RW, Noor AM, Rockett K, Hubbart C, Nankabirwa JI, Greenhouse B, Chang HH, Ghani AC, Verity R. 2021. Evaluating the Performance of Malaria Genetics for Inferring Changes in Transmission Intensity Using Transmission Modeling. *Mol Biol Evol* **38**:274–289. doi:10.1093/molbev/msaa225

WHO. 2012. WHO Policy Recommendation: Seasonal Malaria Chemoprevention (SMC) for Plasmodium falciparum malaria control in highly seasonal transmission areas of the Sahel sub-region in Africa.

WHO/GMP. 2017. A Framework for Malaria Elimination, Geneva World Health Organization.

Wickham H, Averick M, Bryan J, Chang W, McGowan L, François R, Grolemund G, Hayes A, Henry L, Hester J, Kuhn M, Pedersen T, Miller E, Bache S, Müller K, Ooms J, Robinson D, Seidel D, Spinu V, Takahashi K, Vaughan D, Wilke C, Woo K, Yutani H. 2019. Welcome to the Tidyverse. *J Open Source Softw* **4**:1686. doi:10.21105/joss.01686

World Health Organization. 2022. World Malaria Report 2022, World Health Organization. doi:ISBN 978 92 4 1564403

Zhang X, Deitsch KW. 2022. The mystery of persistent, asymptomatic Plasmodium falciparum infections. *Curr Opin Microbiol* **70**:102231. doi:10.1016/j.mib.2022.102231

807 **DATA AVAILABILITY STATEMENT**. The sequences utilized in this study are publicly available in GenBank
808 under BioProject Number: PRJNA 396962. All data associated with this study are available in the main text,
809 the Supporting Information, or upon reasonable request by contacting the Malaria Reservoir Study Team,
810 represented by the corresponding author, Prof. Karen Day (karen.day@unimelb.edu.au), to discuss how
811 these data will be utilized for academic or research purposes and, if appropriate, to explore opportunities
812 for collaboration. All custom code is available in an open source repository: (1) DBLαCleaner pipeline is
813 available athttps://github.com/UniMelb-Day-Lab/DBLaCleaner, (2) clusterDBLalpha pipeline is available at
814 https://github.com/Unimelb-Day-Lab/clusterDBLalpha, and the (3) classifyDBLalpha pipeline is available
815 at https://github.com/Unimelb-Day-Lab/classifyDBLalpha. A dataset to demo this custom code is available
816 at https://github.com/UniMelb-Day-Lab/tutorialDBLalpha**.** For additional information on the use of the
817 Bayesian approach to estimate MOI_{var} please see https://github.com/qzhan321/Bayesian-formulation-
818 varcoding-MOI-estimation.
819
820 **BENEFIT-SHARING STATEMENT**. A research collaboration was developed with scientists from Ghana
821 based at the Navrongo Health Research Centre and the Noguchi Memorial Institute for Medical Research.
822 All collaborators are included as co-authors and the relevant results from the research has been shared
823 with key stakeholders and the local community (i.e., Paramount Chief of Bongo District, divisional Chiefs,
824 Queen Mothers, and community members), the Bongo District and Upper East Regional Health
825 Directorates, as well as Ghana National Malaria Elimination Programme. Before this research was
826 undertaken, informed consent was sought and obtained from the key stakeholders, traditional leadership,
827 and the local community in Bongo District. In addition, members of the local community were trained as
828 field workers and were directly involved in liaising with the community and in the collection of the study

data. The contribution of these individuals to this research is described in the Acknowledgements. This research addresses a priority concern regarding malaria control and the impact of interventions. These concerns are relevant for both the local community in Bongo District, as well as for the National Malaria Elimination Programme in Ghana.

AUTHOR CONTRIBUTIONS. K.P.D and M.P conceptualized the study of population size using MOI_{var}. K.A.K and K.P.D conceived and designed the field study with input from A.R.O and K.E.T, who together with O.B coordinated the field studies. K.E.T, S.R-P, and S.L.D processed the samples and performed the genotyping experiments. G.T-H developed and validated the bioinformatic pipelines. K.E.T, S.R-P, and D.C.A processed, cleaned, and curated the datasets for analysis. Q.Z developed and implemented the Bayesian estimations. K.E.T, Q.Z, M.P, and K.P.D analysed the data with contributions from S.R-P, Q.H, and M-H.T. K.E.T and Q.Z visualized the data. K.P.D, M.P, and K.E.T wrote the original draft of the manuscript. Q.Z., S.R-P, G.T-H, Q.H, M-H.T, D.C.A, S.L.D, O. B, A.R.O, and K.AK reviewed and edited manuscript. M.P and K.P.D supervised the research. A.R.O, K.A.K, M.P, and K.P.D acquired the funding.

COMPETING INTERESTS. The authors declare no competing interests.

FIGURES

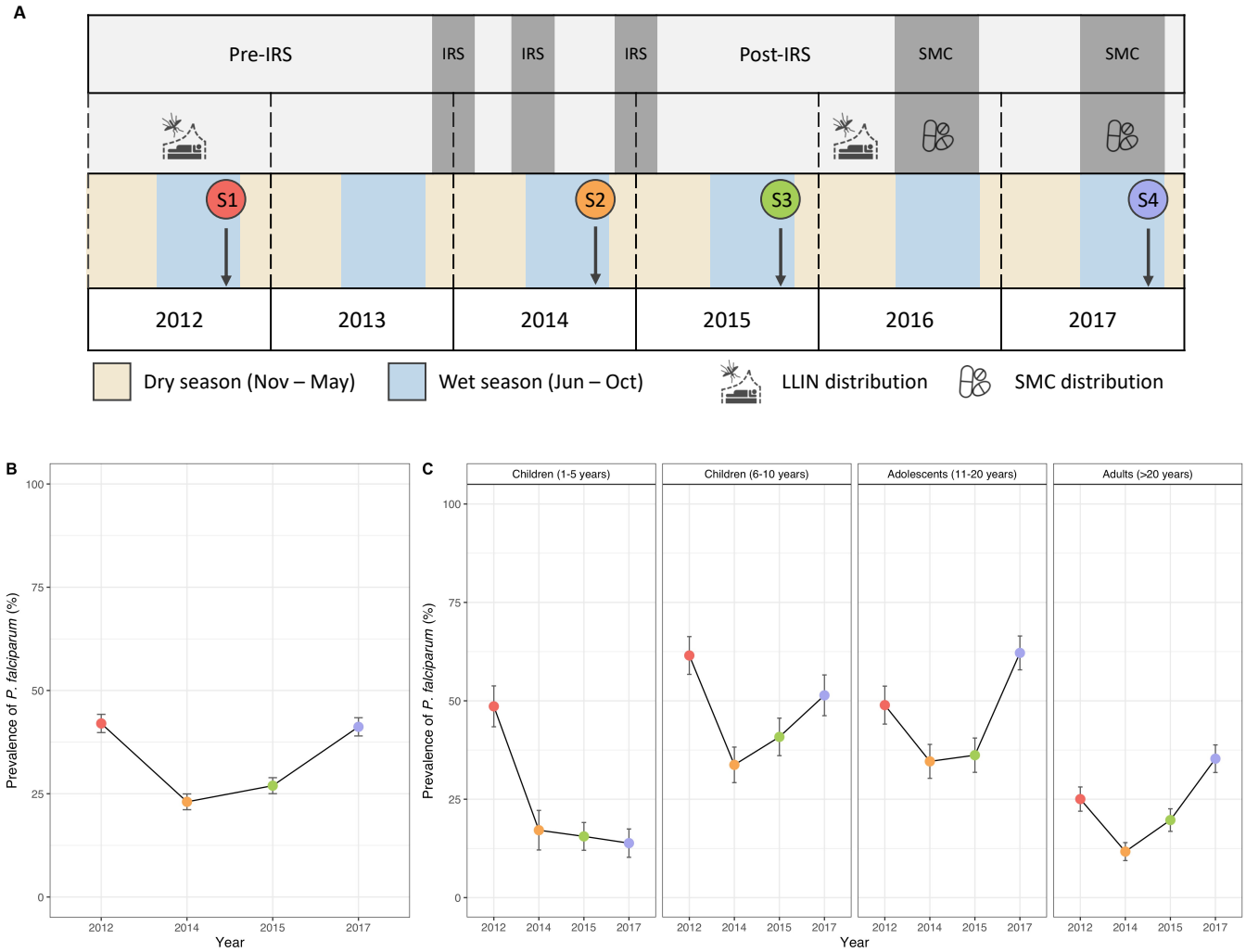

Figure 1. Study design and changes in the prevalence of microscopic *P. falciparum* infection following the IRS and SMC interventions in Bongo, Ghana. (**A**) Four age-stratified cross-sectional surveys of ~2,000 participants per survey were conducted in Bongo, Ghana at the end of the wet seasons in October 2012 (Survey 1, baseline pre-IRS, red), October 2014 (Survey 2, during IRS, orange), October 2015 (Survey 3, post-IRS, green), and October 2017 (Survey 4, SMC, purple) (Table supplement 1) (see Materials and Methods). The three rounds of IRS (grey areas) were implemented between 2013 and 2015 (Tiedje et al., 2022). SMC was distributed to all children < 5 years of age during the wet seasons in 2016 (two rounds between August – September 2016) and 2017 (four rounds between September – December 2017) (Gogue et al., 2020). Both IRS and SMC were implemented against a background of widespread LLIN usage (Tiedje et al., 2022). Prevalence of microscopic *P. falciparum* infections (%) in the (**B**) study population and (**C**) for all age groups (years) in each survey. Error bars represent the upper and lower limits of the 95% confidence interval (CI) calculated using the Wald Interval.

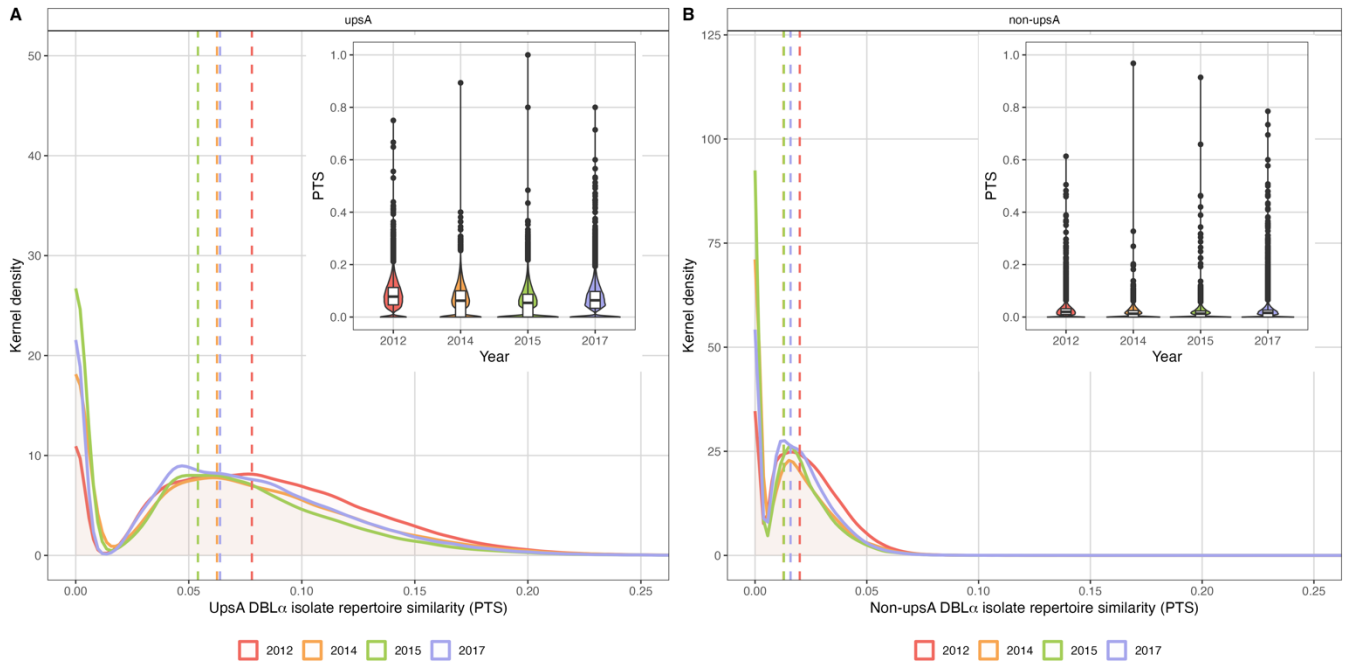

Figure 2. Sharing of upsA and non-upsA DBLα types among the DBLα isolate repertoires in 2012 (pre-IRS, red), 2014 (during IRS, orange), 2015 (post-IRS, green), and 2017 (SMC, purple). The overlapping density and violin plots (upper right-hand corners) show the distribution of PTS scores (i.e., DBLα isolate repertoire similarity) between the (**A**) upsA and (**B**) non-upsA DBLα isolate repertoires for those isolates with DBLα sequencing data (Table supplement 2) in each survey. The PTS scales in the density plots have been zoomed-in to provide better visualization of the upsA and non-upsA DBLα types PTS distributions. The coloured dashed lines in the density plots indicate the median PTS scores in each survey for the upsA (2012 (red) = 0.078, 2014 (orange) = 0.063, 2015 (green) = 0.054, and 2017 (purple) = 0.064) and non-upsA (2012 (red) = 0.020, 2014 (orange) = 0.013, 2015 (green) = 0.013, and 2017 (purple) = 0.016) DBLα types. *Note:* The non-upsA median PTS values in 2014 (orange) and 2015 (green) were both 0.013 and overlap in the figure. In the PTS violin plots the central box plots indicate the medians (centre line), interquartile ranges (IQR, upper and lower quartiles), whiskers (1.5x IQR), and outliers (points).

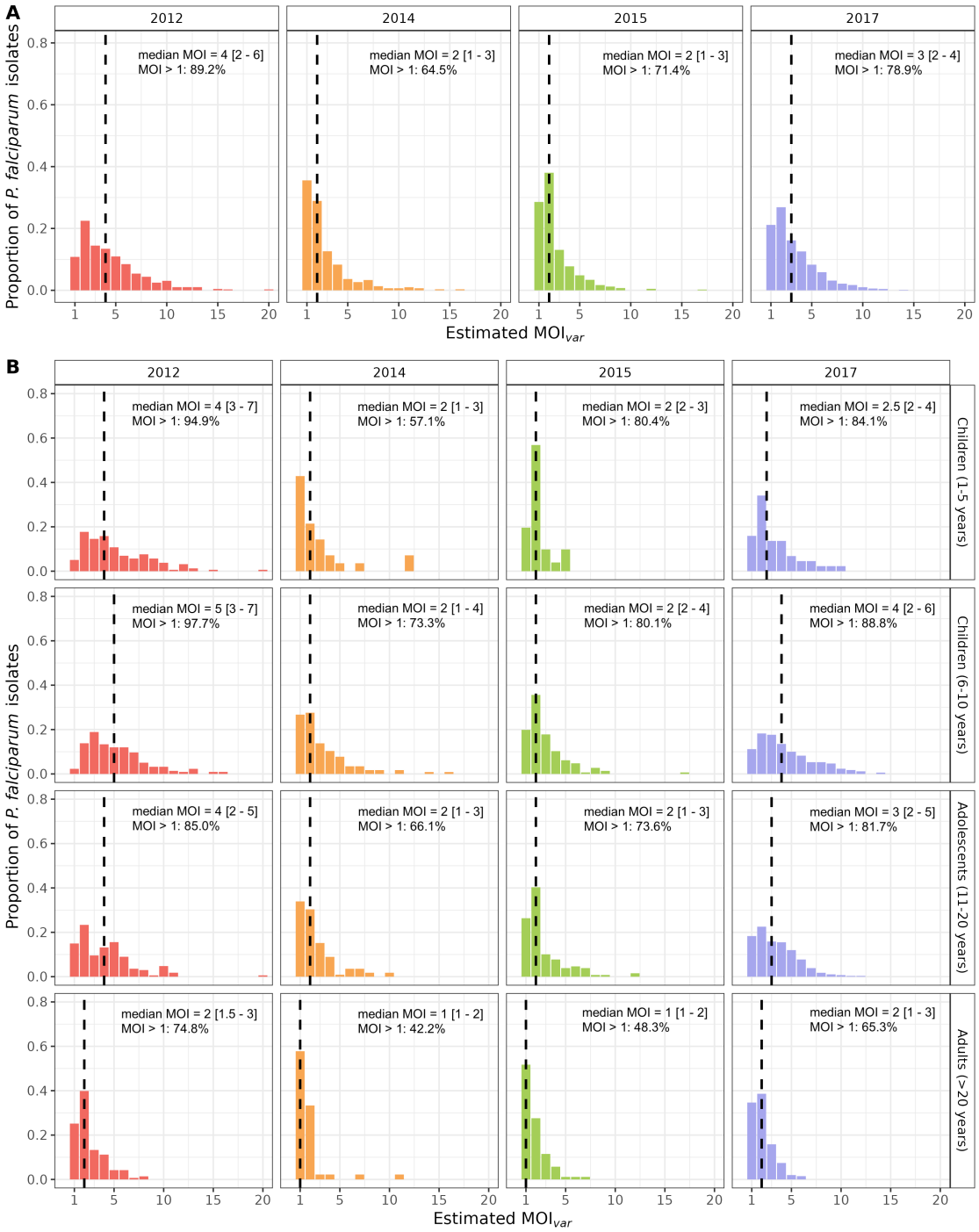

Figure 3. MOI_{var} distributions in 2012 (pre-IRS, red), 2014 (during IRS, orange), 2015 (post-IRS, green), and 2017 (SMC, purple) based on pooling the maximum *a posteriori* MOI estimates. Estimated MOI_{var} distributions for the (**A**) study population and (**B**) for all age groups (years) in each survey for those isolates with DBLα sequencing data (Table supplements 2 and 7). The median MOI_{var} values are indicated with the black dashed lines and have been provided in the top right corner (median MOI_{var} value [interquartile range, upper and lower quartiles]) along with the percentage of *P. falciparum* infections that were multiclonal (MOI_{var} > 1) in each survey and age group (years).

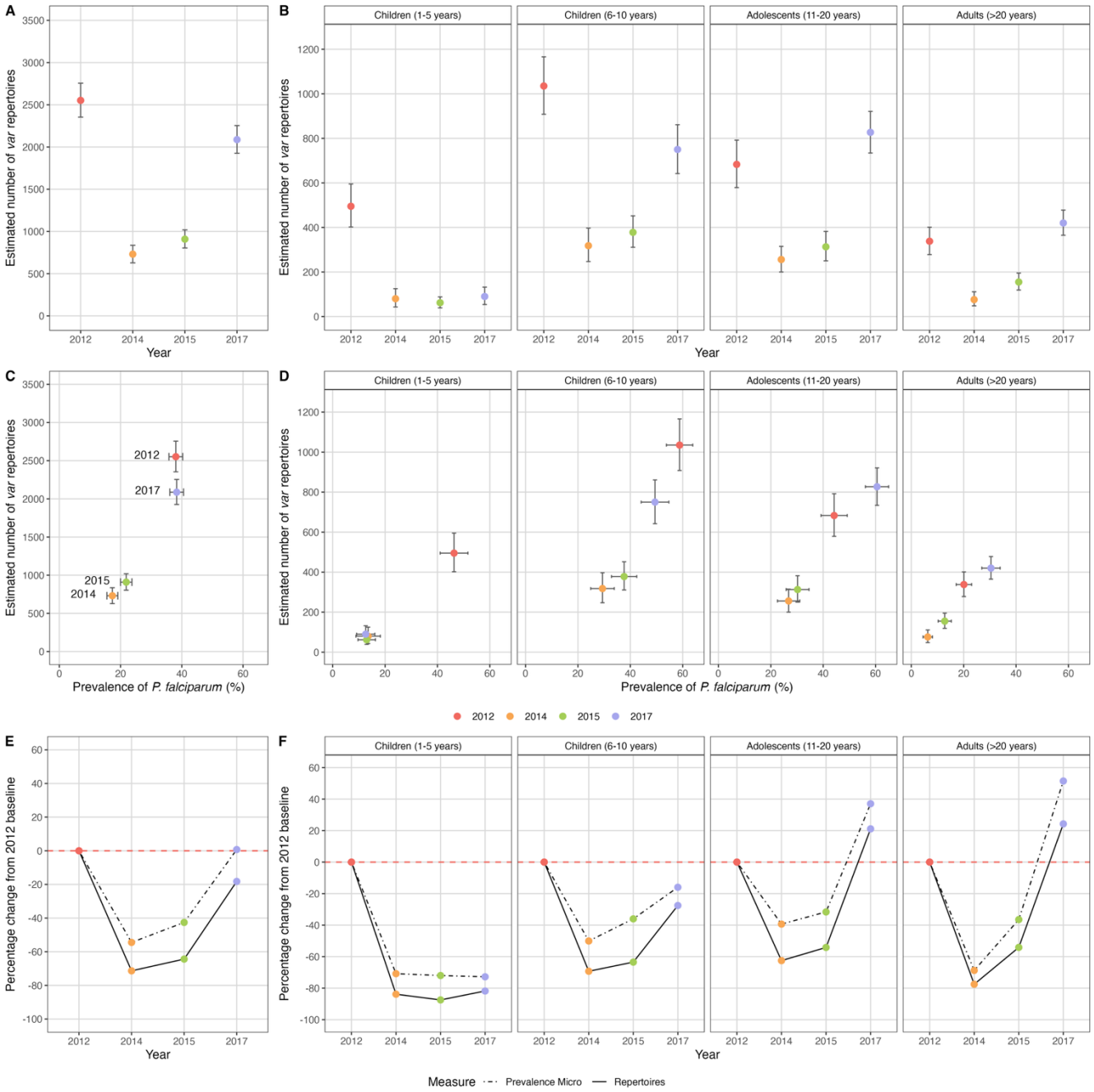

Figure 4. Estimated number and relative change in the number of *P. falciparum var* repertoires in 2012 (pre-IRS, red), 2014 (during IRS, orange), 2015 (post-IRS, green), and 2017 (SMC, purple). The estimated number of *var* repertoires (i.e., census population size) for those isolates with DBLα sequencing data (Table supplements 2 and 7) in the (**A**) study population and (**B**) for all age groups (years). The estimated number of *var* repertoires vs. *P. falciparum* prevalence for (**C**) study population and (**D**) for all age groups (years) (Table supplement 7). The percentage change in *P. falciparum* prevalence (black dotted line) and the estimated number of *var* repertoires (black solid line) in 2014, 2015, and 2017 compared to the 2012 baseline survey (red dashed horizontal line at 0% change) for the (**E**) study population and (**F**)

889 for all age groups (years). Error bars in (**A-D**) represent the upper and lower limits of the 95% confidence
890 intervals (95% CIs). To account for differences in sampling depth across age groups and surveys, we
891 performed subsampling with replacement by selecting the minimum number of individuals in each age
892 group across all surveys. We then calculated the total number of *var* repertoires from these subsampled
893 individuals within each age group in each survey. This approach ensures consistent sample sizes within
894 each age group across all surveys. Finally, we summed the *var* repertoires across age groups to obtain the
895 total *var* repertoire count for each survey. The mean (coloured solid points) and 95% CIs for the number
896 of *var* repertoires were estimated by repeating the subsampling procedure 10,000 times. The CIs were
897 then derived from the distribution of these repeated subsampling replicates. The 95% CIs for *P. falciparum*
898 prevalence (%) were calculated using the Wald Interval.

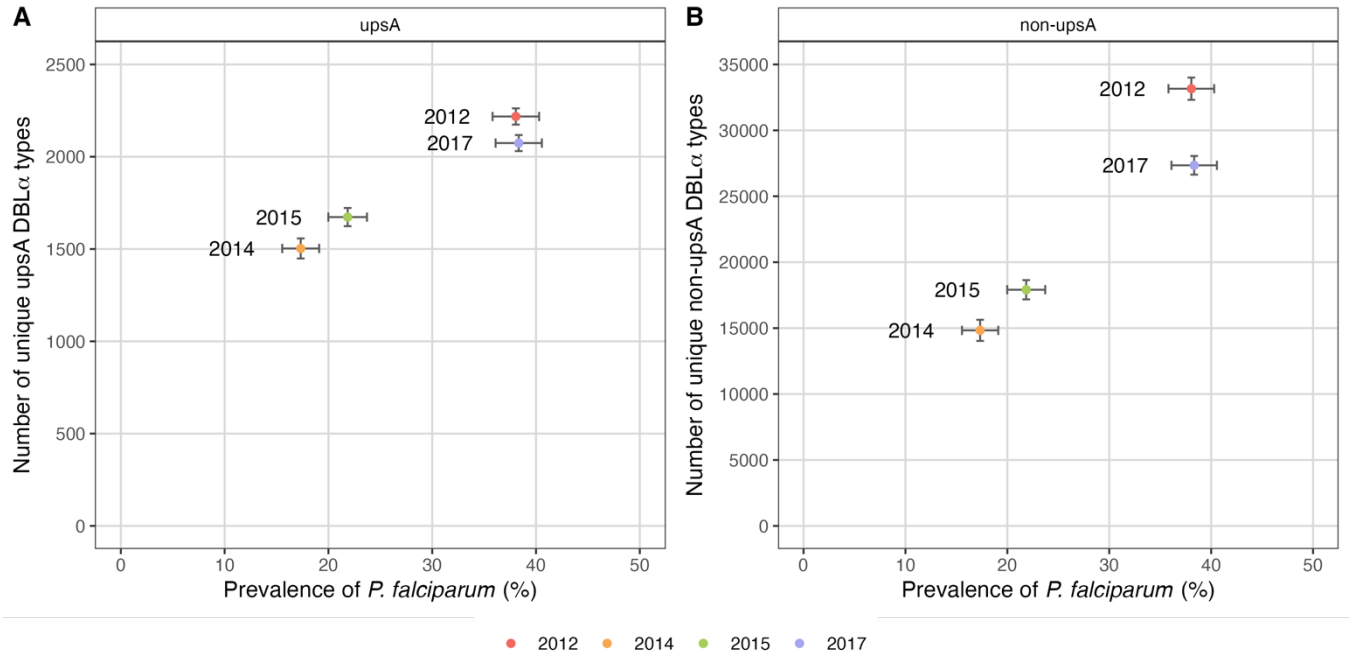

Figure 5. UpsA and non-upsA DBLα type richness in 2012 (pre-IRS, red), 2014 (during IRS, orange), 2015 (post-IRS, green), and 2017 (SMC, purple). Number of unique (**A**) upsA and (**B**) non-upsA DBLα types (i.e., richness) observed in each survey vs. *P. falciparum* prevalence based on those isolates with DBLα sequencing data (Table supplement 2). Error bars represent the upper and lower limits of the 95% confidence intervals (95% CIs) for the *P. falciparum* prevalence (%; x-axis) and ± 2 standard deviations (± 2SD) for the number of unique upsA and non-upsA DBLα types (y-axis). The 95% CIs for *P. falciparum* prevalence (%) were calculated using the Wald Interval. The ± 2SD for the number of unique upsA and non-upsA DBLα types were calculated based on a bootstrap approach. We resampled 10,000 replicates from the original population-level distribution with replacement. Each resampled replicate has the same size as the original sample. We then derive the standard deviation (SD) based on the distribution of the resampled replicates.

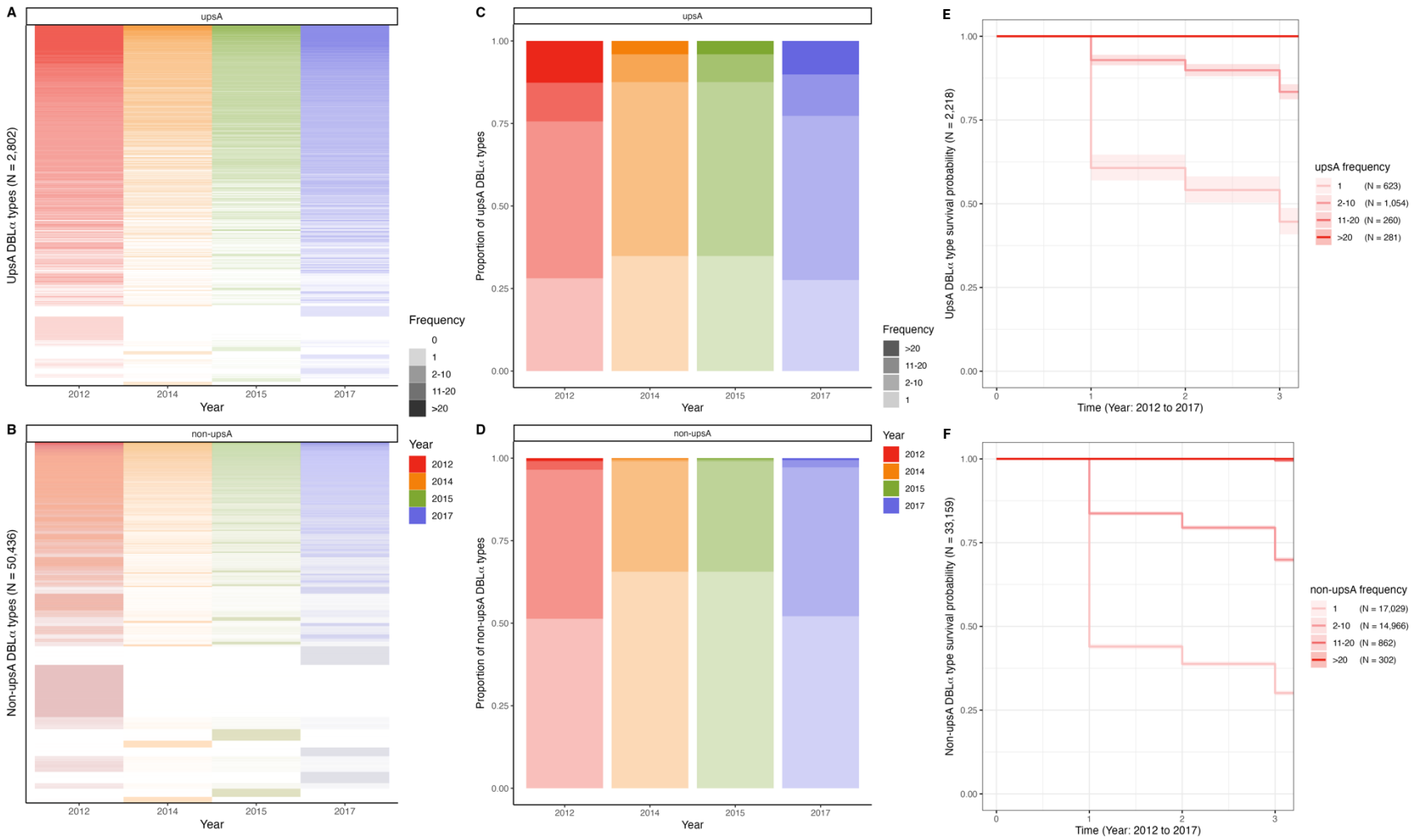

Figure 6. UpsA and non-upsA DBLα type frequencies and survival in 2012 (pre-IRS, red), 2014 (during IRS, orange), 2015 (post-IRS, green), and 2017 (SMC, purple). Heatmaps showing the patterns of diversity for the (**A**) upsA and (**B**) non-upsA DBLα types. The columns represent all the upsA and non-upsA DBLα types observed in the four surveys, and the rows represent each of the 2,802 upsA DBLα types and the 50,436 non-upsA DBLα types (Table supplement 2). White rows are used to denote the absence of a specific DBLα type, while the presence of a DBLα type is indicated in colour and further categorised (colour gradations) based on the frequency or the number of times (i.e., number of isolates) a DBLα type was observed in each survey (Frequency categories: 1, 2-10, 11-20, > 20 isolates;

Note the frequency category cut-offs were chosen based on the frequency distributions in Figure supplement 7). The proportions of (**C**) upsA and (**D**) non-upsA DBLα types in each survey based on the number of times (i.e., number of isolates) they were observed in each survey. Kaplan-Meier survival curves for the (**E**) upsA and (**F**) non-upsA DBLα types across time (2012 to 2017) categorised based on their frequency at baseline in 2012 (pre-IRS, red). The coloured shaded areas represent the upper and lower limits of the 95% confidence intervals (95% CIs) with the number (N) of upsA and non-upsA DBLα types in each frequency category are provided in parenthesis. These survival curves include only those upsA (N = 2,218) and non-upsA (N = 33,159) DBLα types that were seen at baseline in 2012 (pre-IRS) as indicated in red (Table supplement 2). The x-axis indicates time where time "0" denotes 2012 (pre-IRS), "1" denotes 2014 (during IRS), "2" denotes 2015 (post-IRS), and finally "3" denotes 2017 (SMC). *Note:* In the survival curves the 11-20 and > 20 frequency categories for both the (**E**) upsA and (**F**) non-upsA DBLα types overlap in the figure.